

Appendix

Participant Exclusion Criteria

As in our previous analyses which focused on acAN¹, participants of both the recAN and HC groups at the focus of the current analyses were excluded if they had a history of organic brain syndrome, schizophrenia, substance dependence, psychosis NOS, bipolar disorder, bulimia nervosa or binge-eating disorder. Further exclusion criteria included IQ < 85, psychotropic medication within 6 weeks prior to the study (except SSRI; 2 recAN), current substance abuse, inflammatory, neurologic or metabolic illness, chronic medical or neurological illness that could affect appetite, eating behavior, or body weight, clinically relevant anemia, pregnancy or breast feeding.

Image acquisition and processing

Images were acquired from all study participants between 8 and 9 AM following an overnight fast with a Siemens 3T MRI scanner (Erlangen, Germany) equipped with a standard head coil. Structural images were acquired with a T1-weighted MPRAGE sequence (TR=1900 ms, TE=2.26 ms, FOV=256×256 mm, 176 slices, 1×1×1 mm³ voxel size, flip angle=9°). For functional imaging, a standard gradient-echo T₂^{*}-weighted EPI sequence was used (TR=2410 ms; TE=25 ms; flip angle=80°). A total of 636 volumes were obtained (42 transversal slices orientated 17° clockwise to the AC-PC line, 2 mm slice thickness, 1 mm gap, FOV=192×192 mm, in-plane resolution of 64×64 pixels = voxel size of 3×3×2 mm³). Task presentation and behavioral response recording was performed using Presentation software (Neurobehavioral Systems, Inc., Albany, CA).

Imaging data were processed using SPM8 (www.fil.ion.ucl.ac.uk/spm) within

Online appendices are unedited and posted as supplied by the authors.

the Nipype framework (<http://nipy.sourceforge.net/nipype/>). Functional images were slice time corrected, realigned and registered to their mean. The preprocessed images were coregistered to the participant's structural image. A DARTEL template² was created using the structural images from all participants. The functional volumes were normalized to Montreal Neurological Institute (MNI) space using the group template. The resulting data were smoothed with an isotropic Gaussian kernel (8 mm FWHM). Prior to statistical analysis, we evaluated data quality by manual inspection and using artifact detection tools (www.nitrc.org/projects/artifact_detect/) to identify volumes with intensity outliers (> 3 SD from the mean of the time series) and excessive movement (> 2 mm in any direction). The recAN and HC groups at the focus of the current analyses did not differ either in the mean number of volumes per participant with motion [recAN: 4.5(14.9); HC: 3.6(10.4); $t_{70}=.18$; *n.s.*], intensity [recAN: 5.7(4.8); HC: 6.3(4.8); $t_{70}=.42$; *n.s.*] or combined motion and intensity outliers [recAN: .7(1.5); HC: .8(1.6); $t_{70}=.42$; *n.s.*].

Tasks

As in our previous behavioral pilot and fMRI analysis in acAN^{1,3} each trial of the calibration session began with the presentation of a fixation cross (2 s), followed by the delayed larger amount (2 s) and participants indicated their preference with either a left button [for the larger later (LL) alternative] or the right button [for the smaller sooner (SS) option] press. Immediately after a response was given, feedback about the amount and delay chosen was presented (2 s). Participants made 10 decisions for each of the 5 delays. After 10 trials, the delay changed for the next 10 decisions. The calibration session was adaptive such that the rewards displayed increased or decreased based on the subject's decision in the previous trial. For instance, if the immediate amount was chosen, for the next trial the delayed amount increased half the difference between immediate and delayed reward and vice versa.

Online appendices are unedited and posted as supplied by the authors.

To estimate the individual temporal reward discounting parameter k from the choices made during the calibration session as a metric of self-control, we estimated the indifference amount for each of the five delays, i.e. the mean of the maximum delayed amount rejected and the minimum delayed amount chosen. The indifference amount represents the amount A in the hyperbolic function

$$V_d = \frac{A}{1 + k \times D}$$

where V represents the subjective value of a reward, D the delay, and k the individual discount parameter. Parameter k was estimated to best fit the hyperbolic curve consisting of six points, i.e. 20 Euros for no delay (immediate reward) and the indifference amounts of the five delays using ordinary least square.

To individually adapt the intertemporal choices during the imaging experiment on the basis of the individual temporal reward discounting rate k , we computed 18 rewards for each delay (nine with subjective values higher than the individually determined SS option and nine lower) using the following formula:

$$V_d = V_0 \frac{1 + k \times D \times c}{1 + k \times D}$$

where V_0 represents the subjective value of the immediate (zero delay) reward set to one during computation of all delayed subjective values V_d . The parameter c was set to 0.1, 0.15, 0.20, 0.25, 0.30, 0.35, 0.4, 0.45 and 0.50 to ensure that for all subjective values V_d lower than the SS reward the respective delayed amounts were always higher than the immediate ones. To ensure the same range of subjective values for each participant, the maximum value V for each delay was exactly twentyfold the

Appendix 1 to Ehrlich S, King J, Bernardoni F, et al. Intact value-based decision-making during intertemporal choice in women with remitted anorexia nervosa? an fMRI study. *J Psychiatry Neurosci* 2019.

DOI: 10.1503/jpn.180252

Online appendices are unedited and posted as supplied by the authors.

lowest value V for the 180 day D condition (i.e. minimum value for each subject). The difference in subjective values between immediate reward and maximum reward value V was divided into nine equidistant value categories above the immediate reward. The mean of all computed subjective values V was standardized to 30 Euro. Finally, all respective amounts A were computed using the formula

$$A = V_d + (V_d \times k \times D)$$

The intertemporal choices were adapted individually based on the k value estimated in the calibration session so that (1) subjects ought to choose the immediate reward in 50% of trials, (2) the mean subjective value of all delayed rewards would be the same (30 Euro) for each subject, and (3) the maximal subjective value (V) of all rewards was twentyfold the minimum value. The fixed immediate reward was also adapted individually (range: €5 - €15) so that rewards were presented with the same mean over all trials. Sample sets of pairs of amounts (absolute and subjective values) and delays are presented in Appendix Table 1.

Appendix 1 to Ehrlich S, King J, Bernardoni F, et al. Intact value-based decision-making during intertemporal choice in women with remitted anorexia nervosa? an fMRI study. *J Psychiatry Neurosci* 2019.

DOI: 10.1503/jpn.180252

Online appendices are unedited and posted as supplied by the authors.

Appendix Table 1. Sample sets of absolute amounts and subjective values (in brackets) of delayed rewards for two hypothetical participants, one with an individual discount rate of $k=0.0084$ and another one with $k=0.0025$. In one participant the immediate alternative amount was 10.00 Euro (Participant 1), in the other it was 7.00 Euro (Participant 2). As in King *et al.*² the mean subjective value of all rewards was 30.00 Euro for all participants. The mean of all amounts (i.e. absolute values) was 49.55 Euro for Participant 1 and 36.56 Euro for Participant 2. All amounts and respective delays were shown in random order during the fMRI experiment.

10 days		30 days		60 days		120 days		180 days	
Participant 1	Participant 2	Participant 1	Participant 2	Participant 1	Participant 2	Participant 1	Participant 2	Participant 1	Participant 2
10.08 (9.30)	7.02 (6.84)	10.25 (8.19)	7.05 (6.55)	10.50 (6.98)	7.11 (6.16)	11.01 (5.48)	7.21 (5.52)	11.51 (4.58)	7.32 (5.02)
10.12 (9.34)	7.03 (6.85)	10.38 (8.29)	7.08 (6.58)	10.76 (7.15)	7.16 (6.21)	11.51 (5.73)	7.32 (5.61)	12.27 (4.88)	7.48 (5.13)
10.16 (9.38)	7.04 (6.86)	10.50 (8.39)	7.11 (6.60)	11.01 (7.32)	7.21 (6.26)	12.08 (5.98)	7.43 (5.69)	13.03 (5.19)	7.64 (5.24)
10.21 (9.49)	7.04 (6.86)	10.63 (8.49)	7.13 (6.63)	11.26 (7.49)	7.28 (6.30)	12.52 (6.23)	7.53 (5.77)	13.78 (5.48)	7.80 (5.35)
10.25 (9.46)	7.05 (6.87)	10.76 (8.59)	7.16 (6.65)	11.51 (7.65)	7.32 (6.35)	13.03 (6.49)	7.64 (5.85)	14.54 (5.79)	7.96 (5.46)
10.29	7.06	10.88	7.19	11.77	7.38	13.53	7.75	15.29	8.12

Online appendices are unedited and posted as supplied by the authors.

(9.50)	(6.88)	(8.69)	(6.68)	(7.82)	(6.40)	(6.73)	(5.93)	(6.09)	(5.57)
10.34	7.07	11.01	7.21	12.02	7.43	14.03	7.86	16.05	8.28
(9.53)	(6.87)	(8.79)	(6.70)	(7.99)	(6.44)	(6.99)	(6.02)	(6.39)	(5.68)
10.38	7.08	11.13	7.24	12.27	7.48	14.54	7.96	16.81	8.44
(9.57)	(6.90)	(8.89)	(6.73)	(8.16)	(6.49)	(7.24)	(6.10)	(6.69)	(5.79)
10.42	7.09	11.26	7.28	12.52	7.53	15.04	8.07	17.56	8.61
(9.61)	(6.91)	(8.99)	(6.75)	(8.32)	(6.54)	(7.49)	(6.18)	(6.99)	(5.90)
13.55	8.97	15.65	9.42	18.80	10.09	25.11	11.43	31.41	12.76
(12.50)	(8.75)	(12.50)	(8.75)	(12.50)	(8.75)	(12.50)	(8.75)	(12.50)	(8.75)
24.28	20.72	28.04	21.75	33.68	23.29	44.97	26.38	56.26	29.47
(22.39)	(20.20)	(22.39)	(20.20)	(22.39)	(20.20)	(22.39)	(20.20)	(22.39)	(20.20)
35.00	32.47	40.43	34.08	48.56	36.50	64.84	41.34	81.12	46.18
(32.29)	(31.66)	(32.29)	(31.66)	(32.29)	(31.66)	(32.29)	(31.66)	(32.29)	(31.66)
45.72	44.21	52.81	46.41	63.45	49.70	84.71	56.30	105.98	62.89
(42.18)	(43.11)	(42.18)	(43.11)	(42.18)	(43.11)	(42.18)	(43.11)	(42.18)	(43.11)
56.45	55.96	65.20	58.74	78.33	62.91	104.58	71.25	130.83	79.59
(52.07)	(54.57)	(52.07)	(54.58)	(52.07)	(54.57)	(52.07)	(54.57)	(52.07)	(54.57)
67.17	67.70	77.59	71.07	93.21	76.12	124.45	86.2	155.69	96.30
(61.97)	(66.02)	(61.97)	(66.02)	(61.97)	(66.02)	(61.97)	(66.02)	(61.97)	(66.02)
77.90	79.45	89.97	83.40	108.09	89.32	144.32	101.17	180.55	113.01
(71.86)	(77.48)	(71.86)	(77.48)	(71.86)	(77.48)	(71.86)	(77.48)	(71.86)	(77.48)
88.62	91.20	102.36	95.73	122.97	102.53	164.19	116.12	205.40	129.72
(81.75)	(88.93)	(81.75)	(88.93)	(81.75)	(88.93)	(81.75)	(88.93)	(81.75)	(88.93)
99.35	102.94	114.75	108.06	137.85	115.73	184.06	131.08	230.26	146.43
(91.64)	(100.39)	(91.64)	(100.39)	(91.64)	(100.39)	(91.64)	(100.39)	(91.64)	(100.39)

Analysis of decision difficulty

To identify activation associated with decision difficulty as in our previous analyses in acAN¹ and several other dedicated studies^{4–8}, we re-sorted trials according to difficulty (defined in the main article and below) and created a new model with two regressors of interest: easy, hard. Decision difficulty was determined for each participant individually by binning trials into quartiles on basis of the ratio between the immediate reward (i.e. indifference point)/subjective value of the delayed reward. We assumed that decisions in which this ratio fell between the 25th and 75th

Online appendices are unedited and posted as supplied by the authors.

percentile (i.e. trials in which the ratio was ≈ 1) were relatively hard, while all other decisions were relatively easy (i.e. trials in which the ratio was considerably $>$ or $<$ than 1). Confirming the validity of this definition, reaction times on valid trials were faster for “easy” decisions (668 ms) than for “hard” decisions (685 ms) both in the recAN-HC sample at the focus of the current analyses ($F_{1,70}=5.2$; $p < .05$) and in our previous analyses focused on acAN (675 ms vs. 680 ms; $F_{1,61}=3.9$; $p = .05$).

Generalized Psychophysiological Interaction Analysis (gPPI)

To follow up on the results of the decision difficulty analysis in the current analysis focused on the recAN-HC sample which revealed a significant main effect (hard $>$ easy) in the same region of the dACC in which we observed a group difference between acAN and HC (group \times decision difficulty interaction) in our previous study (King *et al.*¹; Figure 3A), we carried out a set of gPPI analyses⁹. Specifically, given the lack of a group difference between recAN and HC in mean hard $>$ easy dACC activation (Figure 3B), we were interested in potential group differences in connectivity between this and other brain regions (“physiological” factor) as a function of decision difficulty (“psychological” factor), both in the recAN-HC sample at the focus of the current article and in the acAN-HC sample originally investigated in King *et al.*¹ (see the following section and Appendix Table 2 for a detailed description of the acAN-HC sample). The seeds for the two gPPI analyses were all voxels belonging to the respective mean activation clusters (hard $>$ easy) in the dACC observed here in the recAN-HC sample (main effect of difficulty; x 6, y 20, z 46; 321 voxels) and previously in the acAN-HC sample¹ (group \times difficulty interaction; x -10, y 30, z 28; 580 voxels) at an uncorrected voxelwise threshold of $p < .005$. On the first level, the physiological activity was obtained by calculating the first eigenvariate across all voxels within the respective seed regions. Next, a whole-

Online appendices are unedited and posted as supplied by the authors.

brain GLM analysis was calculated for each participant using the following regressors: the deconvolved physiological activity of the respective seed region, the psychological factors (hard, easy), and the products of the physiological activity and psychological factors (i.e. PPI regressors). On the second level, the resulting PPI regressors were then contrasted in two independent voxelwise two-sample *t*-tests (acAN vs. HC; recAN vs. HC) to test for group differences in functional connectivity of the dACC as a function of decision difficulty. To control for false-positives, family-wise error (FWE) correction was performed using 3dClustSim as described in the main article.

acAN-HC sample originally included in King *et al.*¹

All data included in the current analyses focused on recAN and our previous analyses focused on acAN² were acquired within our greater fMRI study of delay discounting which took place between 3/2013 and 7/2016. Motivated by the null findings in recAN, we conducted new analysis of the data from the acAN-HC sample originally included in King *et al.*¹. The data were collected from 62 female volunteers (age range: 12 – 22 years): 31 acAN patients diagnosed according to DSM-IV and 31 age-matched HC subjects. acAN patients (80% first episode, i.e. had not previously received adequate treatment and had not yet gained weight) were admitted to eating disorder programs at University Clinic Carl Gustav Carus (Technische Universität Dresden) and underwent scanning within 96 h after beginning nutritional rehabilitation. No acAN patients had received psychotropic medication for at least 6 weeks prior to study participation. Demographic and clinical characteristics of the sample are summarized below in Appendix Table 2. For complete details, see King *et al.*¹.

Table 2. Demographic Variables and Clinical Measures from King et al., 2016

	acAN	HC	<i>t</i>	<i>p</i>
Demographic Variables				
age (years)	15.7 ± 2.5	16.1 ± 2.4	.78	.44
IQ	113.1 ± 11.0	111.9 ± 11.0	0.49	.63
BMI (kg/m ²)	14.7 ± 1.3	20.4 ± 2.0	13.5	< .001
BMI-SDS	-3.1 ± 1.4	-0.08 ± 0.6	10.8	< .001
min. lifetime BMI	14.22 ± 1.23	19.10 ± 1.53	-13.45	< .001
Clinical Measures				
age of onset (years)	13.81 ± 2.06	n.a.	n.a.	-
duration of current episode (months)	14.09 ± 22.7	n.a.	n.a.	-
BDI-II	6.9 ± 5.9	0.6 ± 1.6	5.7	< .001
EDI-2 total	207.4 ± 43.4	152.1 ± 41.0	5.08	< .001
drive for thinness	29.71 ± 8.8	14.85 ± 7.8	7.02	< .001
body dissatisfaction	37.65 ± 10.6	24.03 ± 11.1	4.93	< .001
bulimia	10.74 ± 4.3	10.74 ± 3.5	.80	.996

Mean values ± SD for each variable are shown. BDI-II, Beck Depression Inventory-II; BMI, body mass index; BMI-SDS, body mass index standard deviation scores; EDI-2, Eating Disorder Inventory-2; SCL-90-R, Symptom Checklist-90-Revised. Thirty acAN patients (96.8%) were of the restrictive subtype and 1 (3.2%) were binge/purge. Six acAN patients were diagnosed with comorbid Axis I psychiatric disorders (five depression, three anxiety disorders, one obsessive-compulsive disorder) and one patient received an Axis II diagnosis: avoidant personality disorder.

fMRI region of interest (ROI) analysis

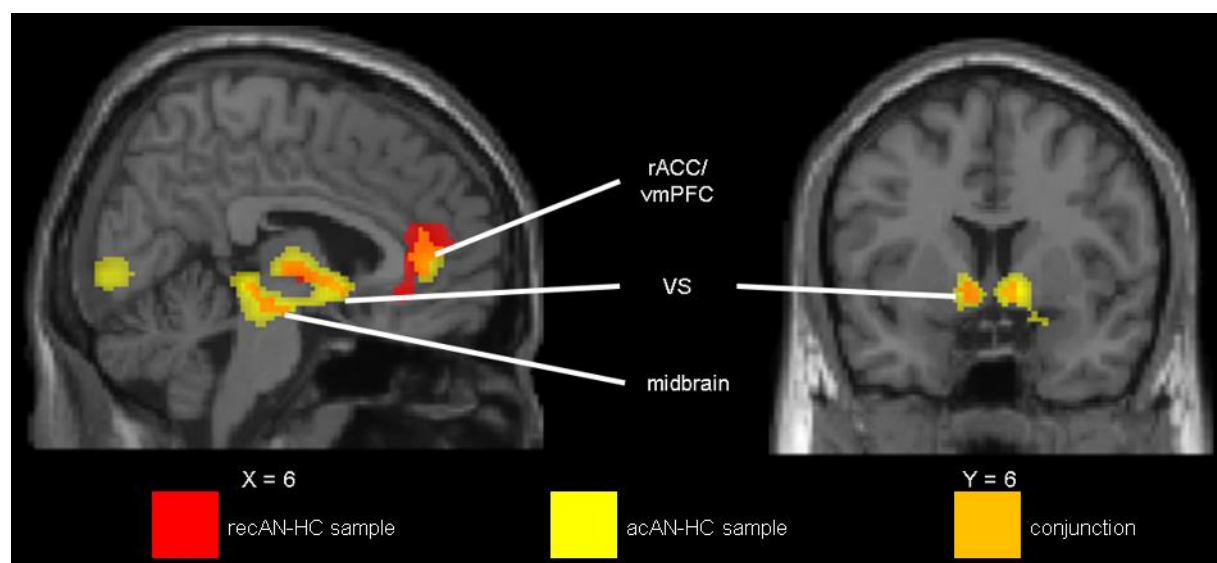
To develop a greater understanding of dACC activation associated with decision difficulty in the recAN-HC sample, we extracted mean β estimates for hard and easy decisions using MarsBaR toolbox for SPM (<http://marsbar.sourceforge.net/>) for each participant from all voxels belonging to the cluster showing a main effect in whole-brain search at an uncorrected voxelwise threshold of $p < .005$ (see Figure 3A) and submitted the data to a 2 (group: recAN, HC) \times 2 (difficulty: easy, hard) repeated-measures ANOVA. The results are depicted in Figure 3B in the main article. We previously used the same analysis procedure to interrogate a group \times difficulty interaction evident in dACC activation in our acAN-HC sample¹ (see also Figure 3A). However, given the age differences between the recAN-HC sample at the focus of the current analyses and the acAN-HC sample included in our previous analyses¹, quantitative comparisons between the two samples would be methodologically problematic. To nonetheless allow for qualitative comparisons of difficulty-related dACC activation between acAN, recAN and HC, age-adjusted activation means for easy and hard decisions for each of the three groups (as obtained from an exploratory group \times difficulty ANCOVA using age as a covariate) are shown for illustrative purposes in Appendix Figure 3.

Supplementary Results

fMRI results

Online appendices are unedited and posted as supplied by the authors.

Confirming that the fMRI experiment elicited activation patterns known from previous studies using the same task^{1,10–12}, one-sample *t*-tests inspecting the main effects of 1) value-dependent processing and 2) executive decision-making indicated an expected significant correlation between the subjective value of the chosen reward and hemodynamic activity in regions thought to play a critical role in processing appetitive stimuli e.g. VS, rostral anterior cingulate cortex/vmPFC^{13,14} (Appendix Figure 1) and elevated activation in regions involved in deliberation between alternative options (e.g. LPFC, PPC, posterior medial frontal cortex) during intertemporal choice^{15,16} (Appendix Figure 2), respectively.

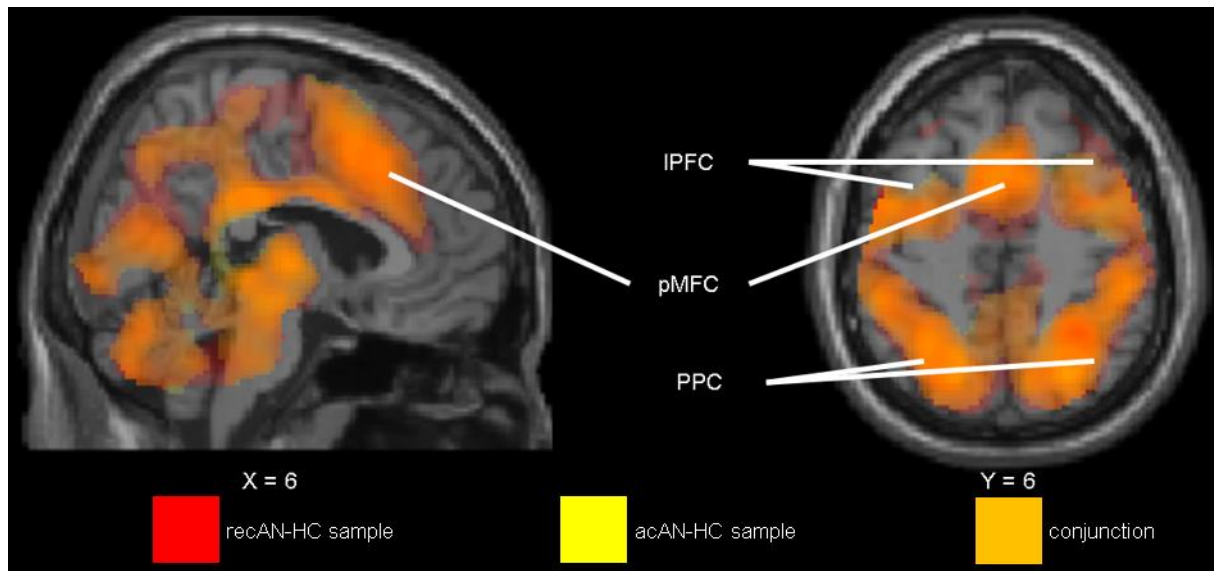


Appendix Figure 1. FWE-corrected ($p < .05$) maps showing regions in which the BOLD signal correlated with subjective value as revealed by one-sample *t*-tests of the respective contrast images (main effect of “value-dependent processing”) from both groups at the focus of the current analyses in the recAN-HC sample (red regions), the acAN-HC sample at the focus of our previous analyses (King *et al.*¹; yellow regions) and their conjunction (orange regions); illustrating the reliability of the analysis to target reward-related brain regions including rostral cingulate cortex/ventrolateral prefrontal cortex (rACC/vmPFC), ventral striatum (VS) and midbrain. This pattern of significant correlation between SV and BOLD activation replicate the results of analog analyses with the same task in independent samples^{10–12} and are consistent with the fMRI literature on intertemporal choice^{15,16}.

Appendix 1 to Ehrlich S, King J, Bernardoni F, et al. Intact value-based decision-making during intertemporal choice in women with remitted anorexia nervosa? an fMRI study. *J Psychiatry Neurosci* 2019.

DOI: 10.1503/jpn.180252

Online appendices are unedited and posted as supplied by the authors.

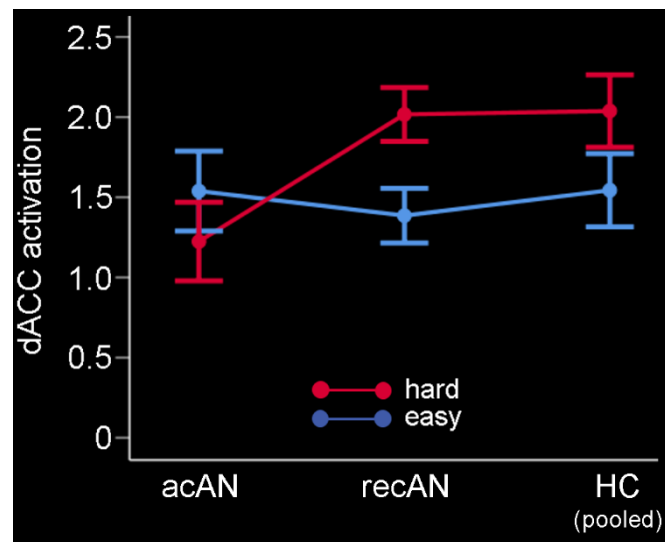


Appendix Figure 2. FWE-corrected ($p < .05$) maps showing regions in which the BOLD activity increased during executive decision-making revealed by one-sample t -tests of the respective contrast images (main effect) from both groups at the focus of the current analyses in the recAN-HC sample (red regions), the acAN-HC sample at the focus of our previous analyses (King *et al.*¹; yellow regions) and their conjunction (orange regions); illustrating the reliability of the analysis to elicit significant activation in brain regions associated with decision-making during intertemporal choice including lateral prefrontal cortex (IPFC), posterior medial frontal cortex (pmMFC) including dorsal anterior cingulate cortex (dACC) and pre-supplementary motor area, and posterior parietal cortex (PPC). These activation patterns replicate the results of analog analyses with the same task in independent samples^{10–12} and are consistent with the fMRI literature on intertemporal choice^{15,16}.

Appendix 1 to Ehrlich S, King J, Bernardoni F, et al. Intact value-based decision-making during intertemporal choice in women with remitted anorexia nervosa? an fMRI study. *J Psychiatry Neurosci* 2019.

DOI: 10.1503/jpn.180252

Online appendices are unedited and posted as supplied by the authors.



Appendix Figure 3. Mean age-adjusted dACC activation on trials with hard and easy decisions (β estimates \pm SEM) is plotted for the acAN sample at the focus of King *et al.*¹ (n=31), the recAN sample at the focus of the current study (n=36) and all HC included in our greater study of delay discounting (n=53).

References

1. King JA, Geisler D, Bernardoni F, et al. Altered Neural Efficiency of Decision Making During Temporal Reward Discounting in Anorexia Nervosa. *J Am Acad Child Adolesc Psychiatry* 2016;55:972–9.
2. Ashburner J. A fast diffeomorphic image registration algorithm. *NeuroImage* 2007;38:95–113.
3. Ritschel F, King JA, Geisler D, et al. Temporal delay discounting in acutely ill and weight-recovered patients with anorexia nervosa. *Psychol Med* 2015;45:1229–39.
4. McClure SM, Laibson DI, Loewenstein G, et al. Separate Neural Systems Value Immediate and Delayed Monetary Rewards', Science, 306, October, 503-7. *Int Libr Crit Writ Econ* 2007;209:282.
5. Jimura K, Chushak MS, Westbrook A, et al. Intertemporal Decision-Making Involves Prefrontal Control Mechanisms Associated with Working Memory. *Cereb Cortex N Y N 1991* 2018;28:1105–16.

Appendix 1 to Ehrlich S, King J, Bernardoni F, et al. Intact value-based decision-making during intertemporal choice in women with remitted anorexia nervosa? an fMRI study. *J Psychiatry Neurosci* 2019.

DOI: 10.1503/jpn.180252

Online appendices are unedited and posted as supplied by the authors.

6. Eppinger B, Heekeren HR, Li S-C. Age Differences in the Neural Mechanisms of Intertemporal Choice Under Subjective Decision Conflict. *Cereb Cortex N Y N 1991* 2017;1–11.
7. Marco-Pallarés J, Mohammadi B, Samii A, et al. Brain activations reflect individual discount rates in intertemporal choice. *Brain Res* 2010;1320:123–9.
8. Koffarnus MN, Deshpande HU, Lisinski JM, et al. An adaptive, individualized fMRI delay discounting procedure to increase flexibility and optimize scanner time. *NeuroImage* 2017;161:56–66.
9. McLaren DG, Ries ML, Xu G, et al. A generalized form of context-dependent psychophysiological interactions (gPPI): a comparison to standard approaches. *NeuroImage* 2012;61:1277–86.
10. Ripke S, Hübner T, Mennigen E, et al. Reward processing and intertemporal decision making in adults and adolescents: the role of impulsivity and decision consistency. *Brain Res* 2012;1478:36–47.
11. Ripke S, Hübner T, Mennigen E, et al. Common neural correlates of intertemporal choices and intelligence in adolescents. *J Cogn Neurosci* 2015;27:387–99.
12. Vetter NC, Steding J, Jurk S, et al. Reliability in adolescent fMRI within two years - a comparison of three tasks. *Sci Rep* 2017;7:2287.
13. Bartra O, McGuire JT, Kable JW. The valuation system: a coordinate-based meta-analysis of BOLD fMRI experiments examining neural correlates of subjective value. *NeuroImage* 2013;76:412–27.
14. Clithero JA, Rangel A. Informatic parcellation of the network involved in the computation of subjective value. *Soc Cogn Affect Neurosci* 2014;9:1289–302.
15. Carter RM, Meyer JR, Huettel SA. Functional neuroimaging of intertemporal choice models: A review. *J Neurosci Psychol Econ* 2010;3:27.
16. Scheres A, de Water E, Mies GW. The neural correlates of temporal reward discounting. *Wiley Interdiscip Rev Cogn Sci* 2013;4:523–45.